Structural features of cross-sectional wing bones in the griffon vulture (Gyps fulvus) as a prediction of flight style

Correlation between wing bone microstructure and different flight styles: The case of the griffon vulture (*gyps fulvus*) and greater flamingo (*phoenicopterus roseus*)

Gian N. Frongia[1]; Salvatore Naitana[1]; Vittorio Farina[1]; Sergio D. Gadau[1] ; Marco D. Stefano[2]; Marco Muzzeddu[3]; Giovanni Leoni[1]; Marco Zedda[1]

[1]Department of Veterinary Medicine, University of Sassari, Italy; [2]Departments of Internal Medicine, Gerontology and Bone Metabolic Disease Section, Molinette Hospital, University of Turin, Italy;[3]Bonassai Breeding and Wildlife Recovery Center, Regional Forest Agency FoReSTAS, Cagliari, Italy

Correspondence
Sergio D. Gadau, Department of Veterinary Medicine, Section of Anatomy, University of Sassari, Via Vienna, 2, 07100 Sassari, Italy.Email: sgadau@uniss.it

Abstract

Flying is the main means of locomotion for most avian species, and it requires a series of adaptations of the skeleton and of feather distribution on the wing. Flight type is directly associated with the mechanical constraints during flight, which condition both the morphology and microscopic structure of the bones. Three primary flight styles are adopted by avian species: flapping, gliding, and soaring, with different loads among the main wing bones. The purpose of this study was to evaluate the cross- sectional microstructure of the most important skeletal wing bones, humerus, radius, ulna, and carpometacarpus, in griffon vultures (*Gyps fulvus*) and greater flamingos (*Phoenicopterus roseus*). These two species show a flapping and soaring flight style, respectively. Densitometry, morphology, and laminarity index were assessed from the main bones of the wing of 10 griffon vultures and 10 flamingos. Regarding bone mineral content, griffon vultures generally displayed a higher mineral density than flamingos. Regarding the morphology of the crucial wing bones involved in flight, while a very slightly longer humerus was observed in the radius and ulna of flamingos, the ulna in griffons was clearly longer than other bones. The laminarity index was significantly higher in griffons. The results of the present study highlight how the mechanics of different types of flight may affect the biomechanical properties of the wing bones most engaged during flight.

KEYWORDS
Bone Microstructure, Flamingo (*Phoenicopterus Roseus*), Flight Style, Griffon Vulture (*Gyps Fulvus*), Wing Skeleton

1. INTRODUCTION

Flight has evolved in birds as a fast and inexpensive locomotion mode involving three-d imensional units of distance (Hedenstrom, 1993; Hedenström et al., 2016; Scacco et al., 2019; Shamoun- Baranes et al., 2016). Evolution led to lightweight skeletons and feathers, pneumatic bones connected to the respiratory system, and high lift- to- weight ratio, making flight an efficient and long- lasting method. Forces generated during flight vary, resulting in different energetic implications for the wing skeleton and producing specific loading patterns that may require anatomical and functional bone adjustments (Chin et al., 2017). Three primary flight styles are used by avian species: flapping, gliding, and soaring. These styles exert different loads among the main wing bones, namely the humerus, the ulna- radius complex, and the carpometacarpal bone (CMC) (Norberg, 1985; Sullivan et al., 2017). During flapping flight, the wings are involved in a continuous up- and- down movement, and they change their attack angle using an ellipsoidal pattern to generate both lift and thrust because of the use of aerobic energy from the pectoral muscles. During gliding flight, the wings stop flapping and are stretched out, producing only a lifting force derived from the potential gravity force. The soaring flight is a type of gliding in which both wings stop flapping and are stretched out; however, the lifting force can derive from ascending thermal air, and the thrust derives from gliding to another ascending thermal air or from orographic uplift air. In both gliding and soaring, the energetic cost is very low (Heers et al., 2016; Henningsson & Hedenström, 2011; Pennycuick, 2002; Richardson et al., 2018; Thielicke & Stamhuis, 2018; Zahedi & Khan, 2007). For birds, the main obstacles during flight are the torsional and bending loads, which impact the feathers and transmit these biomechanical loads to the wing bones in different manners depending on the flight style. Bone microstructural studies can be based on parameters such as the laminarity index (LI), which is the ratio between the number of circular vascular canals and the total number of vascular canals (de Margerie, 2002). The cross- sectional shape, microstructural and mineral density, and LI of wing bones are determined by the interplay between strength and weight, and by the continuous morphological and structural adaptation to the biomechanical loading regimes of flight styles (Carter et al., 1991). Previous studies have proposed that bones with a microstructure consisting of circular canals forming a laminar bone better resist the shear stresses that occur at the bone tissue level in response to torsional loading (de Margerie et al., 2002). De Margerie et al. (2005) analyzed cross sections of

wing bones of 22 avian species, including Falconiformes, Pelecaniformes, and Anseriformes, and observed that torsion- resisting features occurred in wing bones with a high degree of laminarity. This suggests that torsional loads may be the main determinant of the structure of bones. Simons et al. (2011) studied the cross- sectional geometry of forelimb elements within pelecaniform birds with soaring as the primary flight style and observed that the wing bones showed a prevalent circular cross- section and a higher polar moment of area than birds with flap or flap- glide flight styles. Marelli and Simons (2014) compared two species of raptors with similar body size, diet, and habitat and found that the humerus and ulna of the flap- gliding species were more elliptical than those of the static soaring species; this shape may improve resistance to the bending loads associated with a large amount of flapping. A recent study on the most important wing bones of griffon vultures (*Gyps fulvus*, Linnaeus 1758) (static soaring species) showed that ulna and humerus differ in bone mineral density (BMD), LI, and cross- sectional shape compared to CMC (Frongia et al., 2018). This means that differences can be found not only among species with different flight styles, but also among wing bones of the same species. The factors influencing the structural features of wing bones are not fully understood. Some studies (Nudds et al., 2011; Sullivan et al., 2017; Wang et al., 2011) have emphasized the evolutionary aspects of these structural features in particular taxa, whereas others have supported the adaptive aspects of these features (Rensberger & Watabe, 2000; Starck & Chinsamy, 2002; Kuehn et al., 2019; Pratt et al., 2018). Griffon vultures and flamingos (*Phoenicopterus roseus*, Pallas 1811) are poorly studied species. We hypothesize that, compared to griffon vultures, flamingos have a more robust bone structure, higher BMD, and vascular canals oriented in the most efficient direction to face the prevailing forces. Our main objective is to provide information on the structural features of the wing bones of these two genetically different species that also differ in body weight, habitat, food behavior, and flight style. With this, we expect to contribute to the understanding of whether the microstructural features of the wing bones (humerus, radius, ulna, and CMC) are determined by functional aspects in griffon vultures and flamingos.

2 MATERIALS AND METHODS

2.1 Material collection

All experimental procedures were performed in strict accordance with the guidelines of the Ethics Committee of Sassari University, Italy, which approved this study. The study material consisted of humerus, radius, ulna, and carpometacarpus from 10 flamingos (*Phoenicopterus roseus*, Pallas 1811) and 10 griffon vultures (*Gyps fulvus*, Linnaeus 1758). Regarding the flamingo specimens, material was obtained from skeletons of animals that died from natural causes at Molentargius Saline Park, near the city of Cagliari, Italy. The Molentargius marsh covers an area of 550 km and is a very important site for the stopping, wintering, and nesting of many water bird species. It has been protected by the Ramsar Convention since 1977. In addition, the park is a site of community importance (SIC; code ITB 040022). The Molentargius marsh hosts thousands of flamingos and is located along the flyway joining Camargue, France to the Gulf of Gabès, Tunisia (Johnson, 1989; Johnson, 1997; Johnson & Cézilly, 2007). Based on bone morphology, size of the complete skeleton, and feather color (when available), all flamingos were classified as adults. Feathers are typically gray in young individuals and pink in adults because of the carotenoid pigments obtained from crustaceans in their diet (Amat & Rendón, 2017; Zweers et al., 1995). Griffon vulture bones were collected from animals that died after hospitalization at the Department of Veterinary Medicine, University of Sassari, Italy, and at the Rehabilitation Wildlife Center (Bonassai, Regional Agency Fo. Re. S. T. A. S., Italy). These griffon vultures were divided into three age categories: juveniles, subadults, and adults. All griffons were from a colony in northwestern Sardinia near the village of Bosa, with 45- 47 territorial pairs (our personal monitoring 2018).

2.2 Bone preparation

All bones were carefully prepared as previously described (Frongia et al., 2018). Briefly, feathers, skin, remains of muscles, tendons, and ligaments were removed with dissecting instruments. The bones were then treated with powdered enzyme- borax at 75– 80°C for 1 h. After removal of the soft tissues, the bones were dehydrated in an oven at 40°C for 24 h. Once cleaned, the bones were placed in anatomical positions to be photographed.

2.3 Densitometry

Densitometric analysis was performed at the Molinette Hospital (Gerontology and Bone Metabolic Disease Section, Turin, Italy) as previously described (Frongia et al., 2018). Briefly, for each bone, the central area of the midshaft, representing 5% of the total length (L), was scanned using dual- energy X- ray absorption (DXA). The DXA scanner measures areal BMD (mg/cm^2).

2.4 Morphometry

Bones underwent osteometry analysis to estimate length (L) and weight (W) with a digimatic caliper (Mitutoyo, Kawasaki, Japan) and an electronic balance (Kern & Sohn EMB, Balingen - Germany), respectively. This allows the calculation of the brachial index (BI) as the ratio between humerus and ulna length. From each bone, a 1– 2 mm thick ring was sampled using an angular grinder (Telefunken, Berlin, Germany) with a 0.8 mm thick inox disk (Dexter). The central part of the diaphysis (midshaft) was chosen as it is free from tendon and ligament insertions and supports the maximum mechanical stress during flight (Beer et al., 2006). The rings were laid flat, and pictures were taken with a digital camera Canon D650 (Canon, Tokyo, Japan). The following parameters were observed for each sample:

(i) Maximum (Imax) and minimum (Imin) second moment of inertia: this is a significant factor in the determination of flexural stress, shear stress, and deflection for beams, and for critical loads for columns.
(ii) Diaphyseal cavity area (DA).
(iii) Cortical bone area (CA), representing the amount of cortical bone in cross sections.
(iv) Relative cortical area (RCA), which is the ratio between CA and DA indicating resistance to axial compression loading.
(v) Polar moment of inertia (J), also known as second polar moment of area and length standardized polar moment of area, that is the ratio between J and L; this parameter evaluates the resistance to torsional deformation in cylindrical objects.
(vi) Ratio between the second moment of the area in the maximum (Imax) and minimum (Imin) directions, providing information on the shape of cross sections.

All measurements were calculated using ImageJ freeware (version 1.5p, RRID: SCR_003070, NIH, Bethesda, USA) using the BoneJ plugin.

Then, the bone rings were thinned to a 50 µm thickness using grinding paper. Slides were then covered with mounting medium (Eukitt, Merck KGaA, Darmstadt, Germany), photographed with a Zeiss AxioPhot microscope (Carl Zeiss, Wetzlar, Germany), and digitalized using PixeLINK Capture (Navitar, Rochester, New York, USA). The observed vascular canals were classified into four categories based on their direction: longitudinal (l), radial (r), circular (c), and oblique (o). As shown in Figure 5, canals are identified as longitudinal when they run parallel to the long axis, and as radial, circular, and oblique when they are perpendicular (90 ± 22.5°), parallel (0 ± 22.5°), and oblique (45 ± 22.5°) to the bone surface. This classification follows previous literature (de Margerie, 2002; de Ricqlès et al., 1991). For each bone ring, the LI was determined as the ratio between the number of circular canals and the total number of canals (de Margerie, 2002). Furthermore, the exact number and area (ImageJ software) of secondary remiges were estimated in both species, as they attach to the ulna, playing an outstanding role during flight. Each remige was scanned, its area was calculated by tracing an outline around the whole wing, and this was analyzed in ImageJ.

2.5 Statistical analysis

The Kruskal- Wallis test followed by *post hoc* Mann– Whitney pairwise comparison was used to analyze densitometry, LI values, maximum (Imax) and minimum (Imin) second moment of inertia, DA, CA, second moments of area (I), polar moment of inertia (J), and ratio between the second moment of area in the maximum (Imax) and minimum (Imin) direction. Significance was considered at $p < 0.05$.

3 RESULTS

3.1 Densitometry

The statistical analysis revealed significant differences in BMD distribution between the two examined species. The griffon vulture showed a higher density for all bones studied (mean=2.25 mg/cm^2) compared to the flamingo (1.33). Significant differences were found in the bone mineral content between the two species for all bones examined. All values are shown in Table 1. The maximum values observed in griffons and flamingos were in the ulna (2.65) and humerus (1.5 mg/cm^2), respectively (Figure 1).

3.2 Morphometry

The ulna and humerus were the longest and heaviest bones, respectively, examined in both species (Figure 2). Bone lengths (L) and weights (W) are shown in Table 2. The BI (ratio between humerus and ulna lengths) was higher in flamingos (0.959) than in griffon vultures (0.786). The cross sections of the diaphyses showed variable shapes. The radius of flamingos significantly diverged from the other bones examined as it was the most oval in cross section (Figure 3). A significant difference was detected between the radius of both species ($p = 0.0003$), but not between humeri, ulnae, and CMCs. The RCA was

significantly higher in humeri (p = 0.0002) and ulnae (p = 0.0247) of griffons than in those of flamingos, whereas the difference between radii was not significant. CMC was significantly lower in griffon vultures (p = 0.0128) than in flamingos.

FIGURE 1 Bone mineral content (BMC). G, griffon vulture; F, flamingo. **p < 0.001; *p < 0.01

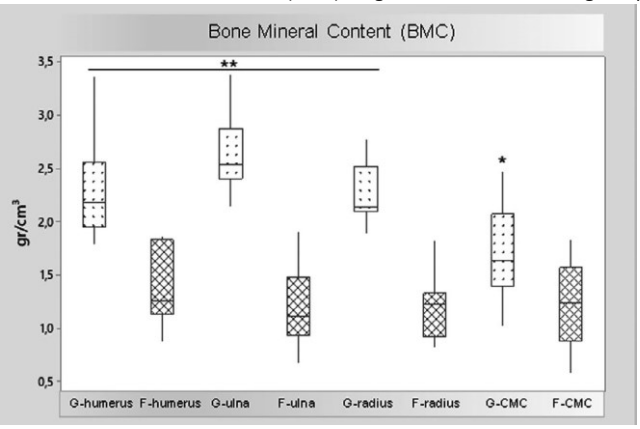

TABLE 1 Means and standard deviation of bone mineral content (BMC) and volumetric bone mineral density (BMD), Imax/Imin, length standardized polar moment of area (J/L), and relative cortical area (CA/TA), from the four main forelimb bones in griffon vulture and flamingo

		BMC (gr)		BMD (gr/cm³)		Imax/Imin		J/L (*10²)		CA/TA	
		mean	*st. dev.*	*mean*	*st. dev.*	*mean*	*st. dev.*	*mean*	*st. dev.*	*mean*	*st. dev.*
Griffon vulture	Humerus	2.581	0.738	2.157	0.711	1.375	0.086	1.791	0.307	0.339	0.056
	Ulna	1.713	0.561	2.491	0.692	1.212	0.055	0.661	0.129	0.398	0.072
	Radius	0.732	0.235	2.131	0.582	1.378	0.161	0.155	0.042	0.415	0.042
	CMC	0.351	0.132	1.598	0.586	1.583	0.189	0.556	0.122	0.338	0.058
Flamingo	Humerus	2.515	0.521	1.345	0.307	1.393	0.142	0.322	0.098	0.214	0.034
	Ulna	1.910	0.506	1.130	0.310	1.212	0.130	0.089	0.026	0.318	0.033
	Radius	0.844	0.171	1.155	0.240	2.204	0.502	0.015	0.006	0.411	0.040
	CMC	0.389	0.127	1.150	0.344	1.481	0.403	0.048	0.019	0.413	0.047

Moreover, the RCA was more homogeneous among the griffon vulture bones than in the flamingo ones, and the radius and CMC showed more variations in flamingos (Table 1; Figure 4). Regarding the length standardized polar moment of area, all griffon vulture bones showed significantly higher values than those of flamingos (Table 1; Figure 5). Humeri had significantly higher values than other bones in both birds (p = 0.0002 in griffon vultures; p = 0.0003 in flamingos). The numbers of secondary remiges in flamingos and griffon vultures were 26 and 20, respectively. Moreover, the mean areas of feathers were 19 cm^2 and 53 cm^2 in flamingos and griffon vultures, respectively (Figure 6). Therefore, the remige area was 2.5 times larger in griffon vultures than in flamingos (3960 vs.
1378 cm^2).

3.3 Laminarity index

Griffon vultures showed significantly decreasing LI values starting from the humerus to the CMC bone (p < 0.001). In contrast, no significant differences among bones were found in flamingos (p = 0.484). The only significant interspecific difference was detected in the humeri, in which LI was higher in griffon vultures than in flamingos (p = 0.002) (Table 3; Figures 7 and 8).

4 DISCUSSION

The evolution of birds consisted of a gradual reduction and loss of skeletal elements, and of the expansion of pneumatized spaces within some bones (Buhler, 1992; Cubo & Casinos, 2000; Dumont, 2010; Fedducia, 1996; Ksepka et al., 2015; Marelli & Simons, 2014; Voeten et al., 2018). The weight of the bird skeleton was reduced to lower metabolic costs while maintaining the strength necessary for flying. This may have been achieved through changes in bone shape and microstructural properties of bone tissue (Muijres et al., 2012; Böhmer et al., 2019). Ontogenetic factors, size, age, and growth rate affect the skeletal microstructure (Kuehn et al., 2019; Skedros et al., 2013). The analysis of the wing bone lengths of griffon vultures and flamingos suggests that the differences between the species can be related to their different flight styles. It is well known that each wing bone exerts a specific function during flight and that its morphology may be linked to biomechanical stress (Kuehn et al., 2019; Schmitz et al., 2018). The humerus and ulna are the main bones involved in flight (Proctor & Lynch, 1993).

4.1 Morphometry

The following strong flight muscles originating from the thorax are attached to the humerus: pectoralis major, supracoracoideus, scapulohumeralis, subcoracoideus, subscapularis, coracobrachialis, and deltoideus (König et al., 2016). These muscles are very robust, and the pectoralis major is the largest muscle in the avian body. It originates from the carina of the sternum, furcula, and sternal ribs, and inserts on the ventral surface of the humerus, which appears as a strong long bone with wide areas for muscle insertion (Proctor & Lynch, 1993). The humerus is a pneumatized bone, and in its diaphysary cavity, some bone bridges connect the inner sides of the shaft, giving strength to the entire bone during flight (Figure 9). The

TABLE 2 Mean and standard deviation of length (L) and weight (W) of the four bones analyzed

	Griffon vulture				Flamingo			
	L (cm)		W (gr)		L (cm)		W (gr)	
	mean	*st. dev.*	*mean*	*st. dev.*	*mean*	*st. dev.*	*mean*	*st. dev.*
Humerus	25.78	1.21	40.52	5.70	20.32	1.09	10.49	2.84
Ulna	32.78	1.27	30.06	5.43	21.18	0.98	6.4	1.75
Radius	31.22	1.21	14.27	2.84	20.74	0.82	2.82	0.67
CMC	13.63	0.56	9.29	1.94	9.37	0.62	2.18	0.62

FIGURE 2 Caudal view of the right wing skeleton in flamingo (a) and griffon vulture (b). The missing portions of the diaphyses were used for histological analysis

FIGURE 3 Cross- sectional shape as ratio between second moment of area in the maximum (Imax) and minimum (Imin) direction. G, griffon vulture; F, flamingo. $^{**}p < 0.001$

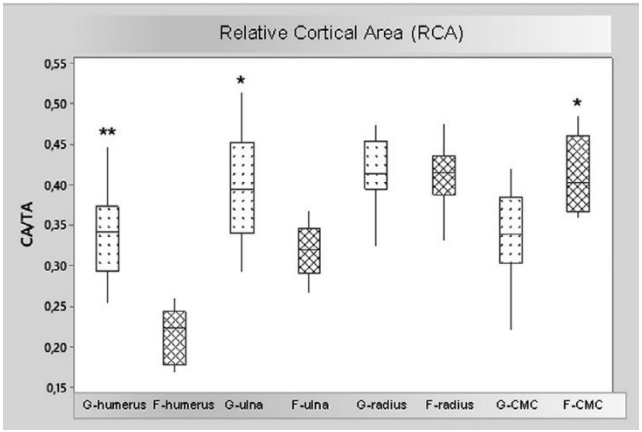

FIGURE 4 Relative cortical area (RCA) as the ratio between cortical bone area (CA) and diaphyseal cavity area (DA). G, griffon vulture; F, flamingo. $^{**}p < 0.001$; $^{*}p < 0.01$

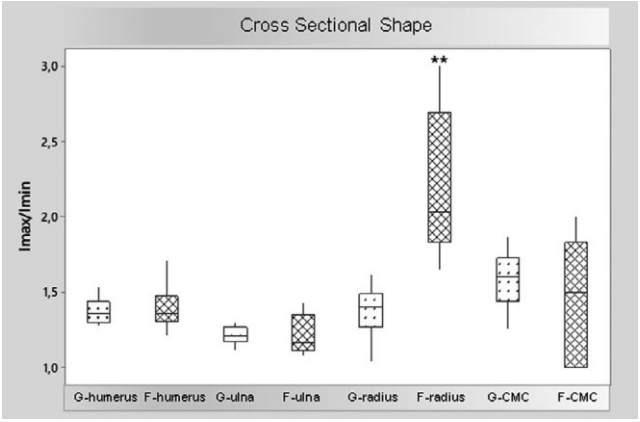

FIGURE 5 Length standardized polar moment of area (J/L). G, griffon vulture; F, flamingo. $^{**}p < 0.001$; $^{*}p < 0.01$

remaining wing muscles are comparatively poorly developed, but they accurately control the position of the remiges and the movements of the forearm and manus bones during flight (Kaiser, 2007). The ulna is the longest bone in the wing and is characterized by the direct attachment of the secondary remiges; thus, its length is related to the number of feathers. The number of secondary remiges in the griffon vulture (20 per wing) is consistent with that reported by Proctor and Lynch (1993; 15– 20 in Accipitridae). Flamingos had 26 feathers as reported in the database (http://www.feath erbase. info). The lengths of the humerus and ulna in both species reflect their flight technique. BI differs among bird groups with different wing strokes during flight (Nudds et al., 2007); high BI (>1.3), medium (1.1– 1.4), and low BI values (<0.80) are typical of flightless.

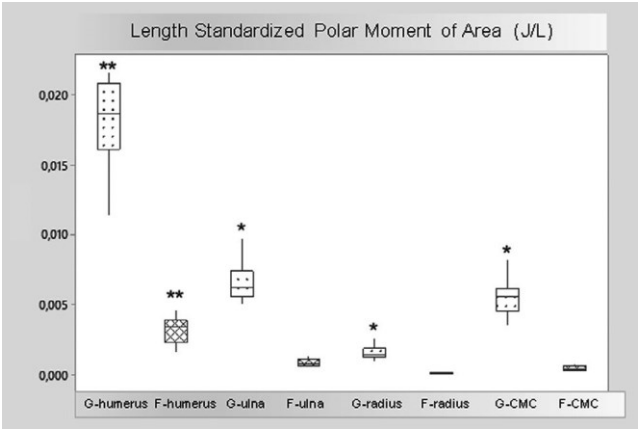

FIGURE 6 Secondary remiges of griffon vulture (a) and flamingo (b)

TABLE 3 Mean and standard deviation of laminarity index (LI) in examined bones birds, underwater swimmers, and strong flapping flyers, respectively. In our study, griffon vultures had lower BI (0.786) than flamingos (0.959; 22% higher). Variations in bone and feather lengths allow different flight styles by altering the joint positions, thus facilitating variations in kinematics (Nudds et al., 2011). The ratio of wing bone length can be used not only to study the different flight styles in living birds, but also to predict the flight styles of fossils. According to Wang et al. (2011), among the three bone wing elements (humerus, ulna/radius, and manus) and primary feathers, the manus length is the poorest predictor for flight style. Wang et al. (2011) also showed the strict correlation between wing elements and flight styles; in particular, the lengths of the humerus and ulna/ radius are good predictors of flight behavior among extant birds. It is worth noting that the length of the humerus and ulna in both bird species reflects their specialization in flight technique. The higher J/L values in griffon vulture bones may be consistent with the stronger mechanical load stressing the wing bones in this species, considering the number of hours that this animal remains in flight in search of food.

	Laminarity index (LI)			
	Griffon vulture		**Flamingo**	
	mean	***st . dev .***	***mean***	***st . dev .***
Humerus	0.50	0.06	0.40	0.05
Ulna	0.48	0.03	0.42	0.08
Radius	0.41	0.05	0.38	0.08
CMC	0.38	0.05	0.39	0.08

FIGURE 7 Laminarity index (LI) of the vascular canals in the bone tissue. G, griffon vulture; F, flamingo. $^{**}p < 0.001$

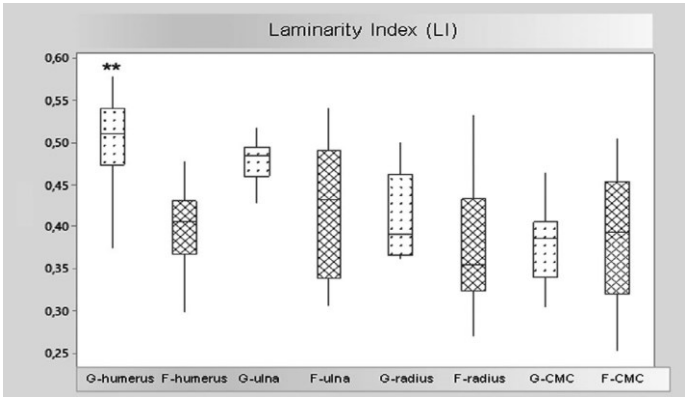

4.2 Influence of flying style on morphometry

Our data show that the length of the radius and ulna in the flamingo are the same and their value is 5% lower than that of the humerus; in contrast, in the griffon vulture, the ulna is approximately 13% longer than the humerus. This means that during flight, the griffon vulture uses its long ulna to glide while reducing energy waste. Indeed, this species is an obligate scavenger that feeds on an unpredictable food supply using the soaring flight to minimize the energetic costs of wide- ranging movements in search of food (Monsarrat et al., 2013; Prinzinger et al., 2002; Ruxton & Houston, 2004). Soaring requires vertical air currents, such as orographic uplifts created by wind currents diverted along mountain ridges or thermals produced over bare land; with this, griffons gain height by circling skywards, increasing their feeding area by gliding (Ellington, 1991; Shamoun- Baranes et al., 2003). Griffons typically fly over land and do not cross even short distances over the sea (Agostini et al., 2005; Bildstein et al., 2009) because of the absence of ascending thermal air currents; with this, they avoid the risk of fatigue during flapping flight and the possibility of drifting off because of crosswinds (Kerlinger, 1989). In contrast, flamingos use their long humerus for flapping, which allows them to cover long distances during migration. The extraordinary flight capability of flamingos has been shown using telemetry, which allowed the tracking of flamingo migrations worldwide (Bechet, 2017; Johnson, 1989, 1997; Sanz- Aguilar et al., 2012). During long- distance flights, flamingos may reach 60– 70 km/h (Childress et al., 2004; McCulloch et al., 2003), or even 90 km/h with supportive winds (Amat et al., 2005). To minimize energy costs, flamingos tend to form rows or V formations, similar to geese (Béchet, 2017), and long- distance flights generally occur at night (Childress et al., 2004). A flamingo leaving Camargue may reach Tunisia 15 h later; with wind support, the journey can last 11 h (Béchet, 2017). A ringed flamingo observed in the afternoon in Camargue was recognized the following day near Oristano, Sardinia, 550 km away (Johnson & Cézilly, 2007). With strong winds, the power of flapping allows flamingos to take off using a single wing beat; when there is no wind, they often need to run on the water surface to take off (Béchet, 2017). On the

FIGURE 9 Transversal section of the humeri of griffon vulture (a, c) and flamingo (b, d). Humeri are the only pneumatized bones of the wing. Note the bone bridges crossing the diaphyseal cavity, which strengthen the whole bone during flight basis of such information, we can suggest that an ulna longer than the humerus, as in griffon vultures, indicates the use of soaring and gliding, whereas a long humerus and ulna, as in flamingos, indicate a flapping flight style. The remarkable length of the griffon ulna must be associated with the area of the secondary remiges (2.5× wider than that of flamingo) (Figure 6). Our data are consistent with the morphology of wing skeletons in wing- propelled diving birds, which represent a model of birds that do not use soaring or gliding flight. In these species (e.g., penguins and auks), underwater propulsion is performed by flapping movements generated by very strong pectoral muscles. Their humerus is almost 30% longer than the radius and ulna (Kaiser, 2007). In contrast, hummingbirds, for instance, have a very short humerus when compared to other wing bones; their flight style can be classified as hovering flight and consists of stroking their wings forward and backward, pivoting up to 180° at the shoulder to rotate the wing. This pattern, with the wingtip tracing an eight- shaped horizontal figure in the air with each wing beat, generates lift on both forward and backward strokes, keeping the bird aloft and allowing it to hover (Warrick et al., 2012). Despite the humerus and radius not being attached to flight feathers, their functions are very different: the humerus transmits all flight loads from the wing to the body, whereas the radius acts as a strut and does receive any direct flight loads

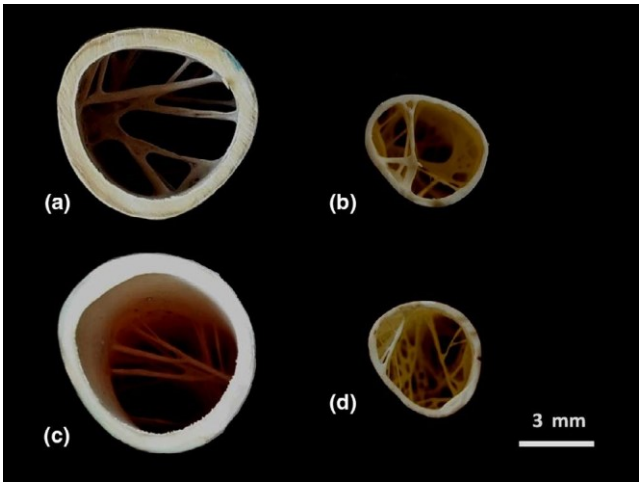

.

FIGURE 8 Histological sections of humerus (a) and ulna (b) of griffon vulture and humerus (c) and ulna (d) of flamingo

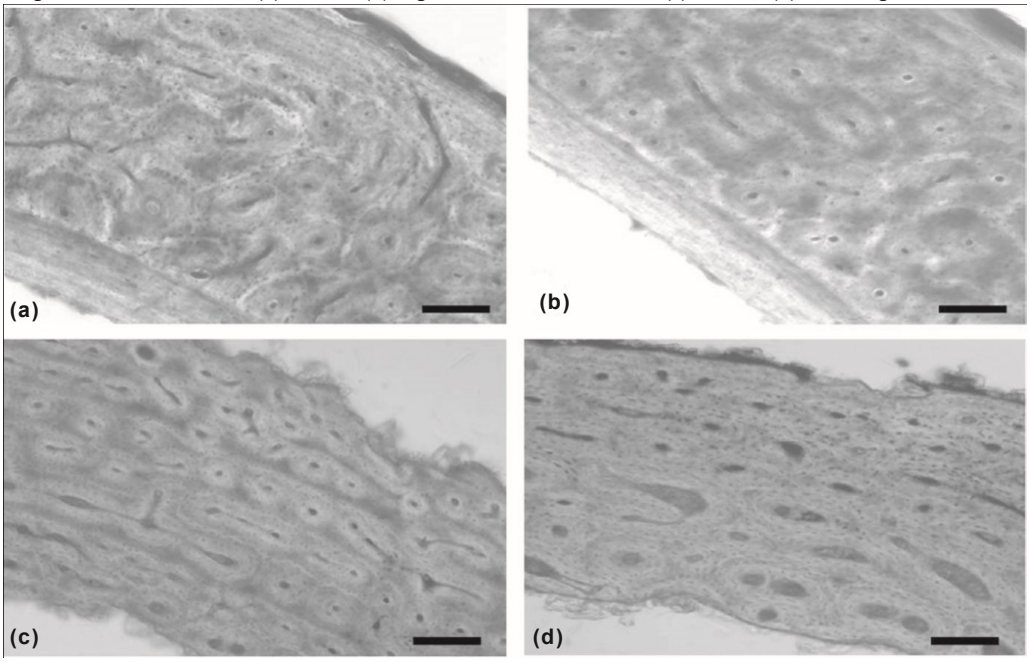

4.3 Bone microstructure and densitometry

Each wing bone has very different loading conditions that may be related to the different flight styles. In addition to length, the importance of the humerus in flamingos and ulna in griffon vultures during flight is represented by our densitometric analysis. The BMD reached its maximum values in the ulna of the griffon vulture and in the humerus in flamingo (Table 1). BMD is strictly correlated with bone stiffness and strength (Currey, 2002, 2003). In the humerus of passerine birds, which perform a very fast flapping flight, a mineral bone density of 2.1 g/cm^3 has been detected (Dumont, 2010), whereas in the humerus of domestic hens, whose wings are not involved in flight, mineral bone density is 0.46 g/cm^3 (Robinson & Karcher, 2019). In the present study, the bone mineral content was higher in griffon vultures than in flamingos (2.25 g/cm^3 and 1.33 g/ cm^3, respectively). This suggests a strong involvement in biomechanical stresses, despite the fact that flamingos fly with active and prolonged flapping wing movements. The less energetic flight of griffons, despite their soaring flight, probably needs higher resistance of wing bones. It is well known that different flight styles require different metabolic costs (soaring <gliding < flapping). Takeoff and landing require a high amount of energy in all bird species. Flamingos use muscle energy, while griffons require bone structures for long flights (6– 9 h/day), for instance, to search for carcasses (Agostini et al., 2015; Bahat, 1998; Bruderer et al., 2010; Duriez et al., 2014; Engel et al., 2006; Norberg, 1990; Norberg, 1996; Nudds & Bryant, 2000; Pennycuick, 2008; Xirouchakis & Andreou, 2009). It can be postulated that this apparent contradiction in griffon vultures is characterized by the soaring flight, which is the flight of lowest cost, and the high BMD of their wing bones could be connected to the fact that their wings face strong resistance during soaring flight. In this regard, it should be highlighted that the highest degree of BMD is in the proximal wing bones (humerus and ulna), which are the skeletal parts most involved in torsion stress. As for the radius, despite it not supporting torsional loads, BMD is significantly high; no data can be found in the literature regarding this matter. Novitskaya et al. (2017) considered the radius and ulna as a unit (radio- ulna unit), arguing that bending and torsional moments supported by the humerus can be transferred to the proximal part of the radius ulna via the elbow joint. Therefore, as it is integral to the ulna, the radius could indirectly experience some degree of torsion, and this could explain the BMD we detected. Muscular resistance to the torsional biomechanical stress occurring during soaring flight is very important to stabilize the position of the secondary remiges. This assertion agrees with the fact that the primary remiges that insert into the hand skeleton are often positioned upwards during the soaring flight as the distal part of the wing is weakly involved in contrasting the torsion stress. The suppleness of some primary remiges on the wingtips of large soaring birds, such as griffon vultures, allows the reduction of air vortices, providing more stability to the wingtips (Baufrère, 2009; Dvořàk, 2016). This last movement of the last remiges on the wingtips, which characterize vultures worldwide, is particularly evident during the landing maneuver, when a great precision of movements is required (Dhawan, 1991). In flamingos, the need to contrast torsion stress is less evident than in griffon vultures. Therefore, BMD is lower in flamingos, and all of the wing skeletal parts are involved, especially in flipping flight. Indeed, in flamingos, the primary remiges are aligned with the others. They are the longest and narrowest feathers in the wing, and they are very important for flapping flight, sourcing the thrust to move the bird body forward through the air (Wang & Meyers, 2017). Primary remiges are inserted in the carpometacarpus and phalanges, which explains the higher BMD value of these bones in flamingos than in vultures. Wing bones must be light to limit the metabolic cost of flying while being strong enough to withstand the loads developed during flight. Wing bone density expresses the mineral content, reflecting a positive interaction with bone stiffness and negative interaction with toughness (Dumont, 2010). If this is true, the lower mineral density of flamingo bones could confer more ductility than that of griffons, ensuring a better

answer to dynamic flight in the former species. Furthermore, it can be suggested that different bone densities are associated with flight style as an adaptation in avian species. The bone density data herein reported suggest that griffon wing bones are, on average, stronger and stiffer than flamingo bones. The higher value of mineral density in griffons could be determined by a greater need to resist twisting than in flamingos. In our previous study (Frongia et al., 2018), we showed that the CMC had a significantly lower mineral density than the humerus and ulna, as the latter bones must resist torsion loads. CMC was therefore attributed to resisting bending loads. The high BMD values detected in vulture wing bones may be due to the considerable torsional and bending stresses that this species must support.

4.4 Laminarity index and flight style

Bone laminarity can be influenced by various factors, such as age, growth rate, and phylogenetic relationship (Padian, 2013). Although some studies have shown that growth rate and phylogenetic aspects have greater impact on bone LI than biomechanical aspects related to torsion forces, it should be noted that these studies were performed using bones of the hind limb of terrestrial species, such as emus and penguins (Ksepka et al., 2015; Kuehn et al., 2019; de Mergerie et al., 2004). In contrast, other studies have shown that biomechanical aspects, such as torsional forces, can have an important role in LI (de Margerie, 2002). Our data indicate that different torsional forces seem to act in different flying styles, as shown by de Margerie (2002). Indeed, this bone microstructural parameter may be correlated to the capability of resisting torsion stresses, whereas bones that predominantly experience compression, tension, or bending forces have a lower LI (de Margerie, 2002; de Margerie et al., 2005; Skedros & Hunt, 2004). LI was higher in all examined bones of griffon vultures than in those of flamingos, demonstrating the former species' great ability to contrast the torsion strength during soaring flight. This may result from the overall shape of their wings, which are broad and large, leading to a great torsional moment. In contrast, the flamingo wing is thin and elongated, and its area is 2.5 times smaller than that of the griffon vulture. Similar observations on LI and flight style have been described for three bird species: pelicans (perform static soaring), cormorants (continuous flapping), and albatrosses (dynamic soaring) (Simons & O'Connor, 2012); the albatrosses exhibited a lower LI in the humerus, ulna, and carpometacarpus than pelicans and cormorants. Although the differences among the bones of each species are slightly larger in our study, the results herein shown agree with those of Simons and O'Connor (2012). In the griffon vulture, LI significantly decreased from the humerus to the CMC, whereas all bones had similar LI in the flamingo. Once again, the microstructural data suggest a greater involvement of the humerus, radius, and ulna of griffon vultures, in contrast to the torsion strength. LI is different among the griffon wing bones, with the humerus and ulna showing significantly higher values than the radius and CMC. In the flamingo, the LI values almost overlap, suggesting that all wing bones in flamingos answer similarly to the bending and torsion loads. The higher LI shown by the griffon's humerus compared to the flamingo's humerus suggests the greater torsion- resistant features of the former species (de Margerie et al., 2005). In contrast to flamingos, vultures are obligate scavengers adapted to static soaring. Low- cost flight is necessary for griffons to identify perishable food, particularly during spring to feed their offspring (Ruxton & Houston, 2004). Our data showed that, considering all wing bones, the griffon showed a higher relative polar moment of area than the flamingo, confirming the influence of this parameter in soaring birds. Among all wing bones, the humerus showed a considerably higher level of polar moment, contributing more than other bones to resist torsion loads. Similarly, the amount of cortical bone in the cross- section can be used to estimate the axial skill compression of bones, revealing higher values in both humerus and ulna in griffons than in flamingos. It is known that a more circular cross- section of wing bones has higher resistance to torsional loads. Simons et al. (2011) observed that pelecaniform birds' wing bones (soaring birds) have a circular cross- sectional shape, different from that of flapping or flap- glide birds. The flamingo radius showed a significantly elliptical cross- sectional shape compared to that of griffons. No significant differences were observed between the CMC of both species, while the griffon's CMC was more elliptical than that of other birds. The widely used analysis of LI using traditional histological examination is limited, so we tried to extrapolate data of three- dimensional structures from two-d imensional histological sections. Recently, Pratt and Cooper (2017) used micro- CT to evaluate the three- dimensionality of the vascular channels of the bone with great precision. This method should be used together with traditional histological examination to better evaluate the actual histological structure of bones.

5 CONCLUSIONS

Our results demonstrate that both flamingo and griffon, while having different flight styles, show the same circular cross- sectional shape of the humerus and ulna, which are adapted to resist torsion loads. The differences in flight style between these two species are due to the higher elliptical cross- sectional shape of the radius in the flamingo and of the CMC in the griffon, compared to other wing bones. In conclusion, following the principles of phylogeny and adaptation to explain the differences or analogies in the corresponding morphological structures of the wing bones, we observed that griffon wing bones can withstand much higher forces than those of the flamingo, indicating an adaptation to the torsional and flexural loads acting on the wings. The fact that adaptability and not phylogeny is the most probable explanation for the differences observed between both species is supported by the finding that the flamingo wing bones are not as strong as the griffon ones. Further studies including multiple species are warranted to separate the phylogenetic effects from the adaptation effects.

ACKNOWLEDGMENTS

The authors wish to thank Dr. L. Massa, from Molentargius Saline Park, for her support during flamingo skeleton sampling.

AUTHOR CONTRIBUTIONS

GNF and SN designed the study. GNF performed statistical evaluations and with VF and MZ acquired bone measurements and performed all the morphological evaluations. SDG drafted both graphics and images. MDS performed the mineral content analysis of the bones. MM helped in the griffon skeleton sampling. GL performed some statistical evaluations. MZ coordinated the work team and the final draft of the manuscript. SN, VF, SDG, and MZ wrote the final version of the manuscript.

DATA AVAILABILITY STATEMENT

The data that support the findings of this study are available from the corresponding author upon reasonable request.

ORCID

Salvatore Naitana https://orcid.org/0000-0001-7601-5952 Sergio D. Gadau https://orcid.org/0000-0001-8579-3799

REFERENCES

Agostini, N., Panuccio, M. & Pasquaretta, C. (2015) Morphology, flight performance, and water crossing tendencies of Afro- Palearctic raptors during migration. *Current Zoology*, 61, 951– 958.

Agostini, N., Premuda, G., Mellone, U., Panuccio, M., Logozzo, D., Bassi, E. et al. (2005) Influence of wind and geography on orientation behavior of adult honey buzzards Pernis apivorus during migration over water. *Acta Ornithologica*, 40, 71– 74. https://doi. org/10.3161/068.040.0101

Amat, J.A. & Rendón, M.Á. (2017) Flamingo coloration and its significance. In: Anderson, M.J. (ed) *Flamingos, Behavior, Biology, and Relationship with Humans*. New York NY: Nova Science Publishers, chap. 4, pp. 77– 95.

Amat, J., Rendón, M.Á., Rendón- Martos, M., Garrido, A. & Ramírez, J.M. (2005) Ranging behaviour of greater flamingos during the breeding and post- breeding periods: Linking connectivity to biological processes. *Biological Conservation*, 125, 183– 192.

Bahat, O. (1998) Long- range movements of griffon vultures from Israel.

Torgos, 28, 19– 23.

Baufrère, H. (2009) A review of biomechanic and aerodynamic considerations of the avian thoracic limb. *Journal of Avian Medicine and Surgery*, 23, 173– 185.

Béchet, A. (2017) Flight, navigation, dispersal, and migratory behavior. In: Anderson, M.J. (ed) *Flamingos: behavior, biology, and relationship with humans*. New York, NY: Nova Science Publishers, chap. 5, pp. 97– 106, ISBN: 978- 1- 53610- 236- 239.

Beer, F.P., Johnston, E.R. & DeWolf, J.T. (2006) *Mechanics of materials*. Boston: McGraw- Hill Higher Education.

Bildstein, K.L., Bechard, M.J., Farmer, C. & Newcomb, L. (2009) Narrow sea crossings present major obstacles to migrating griffon vultures *Gyps fulvus*. *Ibis*, 151, 382–391.

Böhmer, C., Plateau, O., Cornette, R. & Abourachid, A. (2019) Correlated evolution of neck length and leg length in birds. *Royal Society Open Science*, 6, 181588. https://doi.org/10.1098/rsos.181588. eCollection.

Bruderer, B., Peter, D., Boldt, A. & Liechti, F. (2010) Wing- beat characteristics of birds recorded with tracking radar and cine camera. *Ibis*, 152, 272– 291.

Buhler, P. (1992) *Light bones in birds*. Los Angeles CA: Natural History Museum of Los Angeles, Science Series, 36, 385– 394.

Carter, D.R., Wong, M. & Orr, T.E. (1991) Musculoskeletal ontogeny, phylogeny, and functional adaptation. *Journal of Biomechanics*, 24(Suppl1), 3– 16.

Childress, B., Harper, D., Hughes, B., van den Bossche, W., Berthold, P. & Querner, U. (2004) Satellite tracking lesser flamingo movements in the Rift Valley, East Africa: pilot study report. *Ostrich*, 75, 57– 65.

Chin, D.D., Matloff, L.Y., Stowers, A.K. Tucci, E.R. & Lentink, D. (2017) Inspiration for wing design: how forelimb specialization enables active flight in modern vertebrates. *Journal of the Royal Society, Interface*, 14, 1– 18.

Cubo, J. & Casinos, A. (2000) Incidence and mechanical significance of pneumatization in the long bones of birds. *Zoological Journal of the Linnean Society*, 130, 499–510.

Currey, J.D. (2002) *Bones: structure and mechanics*. Princeton NJ: Princeton University Press.

Currey, J.D. (2003) The many adaptations of bone. *Journal of Biomechanics*, 36, 1487– 1495. de Margerie, E. (2002) Laminar bone as an adaption to torsional loads in flapping flight. *Journal of Anatomy*, 201, 521– 526.

de Margerie, E., Cubo, J. & Castanet, J. (2002) Bone typology and growth rate: testing and quantifying 'Amprino's rule' in the mallard (*Anas platyrhynchos*). *Comptes Rendus Biologies*, 325, 221– 230.

de Margerie, E., Robin, J.P., Verrier, D., Cubo, J., Groscolas, R. & Castanet, J. (2004) Assessing a relationship between bone microstructure and growth rate: a fluorescent labelling study in the king penguin chick (Aptenodytes patagonicus). *Journal of Experimental Biology*,

207, 869– 879. https://doi.org/10.1242/jeb.00841 de Margerie, E., Sanchez, S., Cubo, J. & Castanet, J. (2005) Torsional resistance as a principal component of the structural design of long bones: comparative multivariate evidence in birds. *The Anatomical Record Part A: Discoveries in Molecular, Cellular, and Evolutionary Biology: An Official Publication of the American Association of Anatomists*, 282, 49– 66.

Dhawan, S. (1991) Bird flight. *Sadhana*, 16, 275– 352.

Dumont, E.R. (2010) Bone density and the lightweight skeletons of birds. *Proceedings of the Royal Society B: Biological Sciences*, 277, 2193– 2198.

Duriez, O., Kato, A., Tromp, C., Dell'Omo, G., Vyssotski, A.L., Sarrazin, F. et al. (2014) How cheap is soaring flight in raptors? A preliminary investigation in freely- flying vultures. *PLoSOne*, 9, e84887.

Dvořàk, R. (2016) Aerodynamics of bird flight. *EPJ Web of Conferences*, 14, 1– 8. https://doi.org/10.1051/epjco nf/20161 1401001

Ellington, C.P. (1991) Limitations on animal flight performance. *Journal of Experimental Biology*, 160, 71– 91.

Engel, S., Biebach, H. & Visser, G.H. (2006) Metabolic costs of avian flight in relation to flight velocity: a study on rose coloured starling (Sturnus roseus, Linnaeus). *Journal of Comparative Physiology B*, 176, 415. https://doi.org/10.1007/s0036 0- 006- 0063- 1

Fedducia, A. (1996) *The origin and evolution of birds*. New Haven CT: Yale University Press.

Frongia, G.N., Muzzeddu, M., Mereu, P., Leoni, G., Berlinguer, F. & Zedda, M. et al. (2018) Structural features of cross- sectional wing bones in the griffon vulture (*Gyps fulvus*) as a prediction of flight style. *Journal of Morphology*, 279, 1753– 1763.

Hedenstrom, A. (1993) Migration by soaring or flapping flight in birds: the relative importance of energy cost and speed. *Philosophical Transactions of the Royal Society B*, 342, 353– 361. https://doi. org/10.1098/rstb.1993.0164

Hedenström, A. & Åkesson, S. (2016) Ecology of tern flight in relation to wind, topography and aerodynamic theory. *Philosophical Transactions of the Royal Society B: Biological Sciences*, 371, 20150396. https://doi.org/10.1098/rstb.2015.0396

Heers, A.M., Baier, D.B., Jackson, B.E. & Dial, K.P. (2016) Flapping before Flight: High Resolution, Three- Dimensional Skeletal Kinematics of Wings and Legs during Avian Development. *PLoS One*, 11, e0153446.

Henningsson, P. & Hedenström, A. (2011) Aerodynamics of gliding flight in common swifts. *The Journal of Experimental Biology*. 214, 382- 393.

Johnson, A.R. (1989) Movements of greater flamingos (*Phoenicopterus ruber roseus*) in the Western Palearctic. *Revue d Ecologi (Terre Vie)*, 44, 75– 94.

Johnson, A.R. (1997) *Phoenicopterus ruber* Greater Flamingo. *BWP Update*, 1, 15– 23.

Johnson, A.R. & Cézilly, F. (2007) *The Greater Flamingo*. London: T & AD Poyser.

Kaiser, G.W. (2007) *The inner bird – Anatomy and evolution*. Vancouver, Toronto: UBC Press.

Kerlinger, P. (1989) *Flight Strategies of Migrating Hawks*. Chicago IL:
University of Chicago Press.

Ksepka, D.T., Werning, S., Sclafani, M. & Boles, M.Z. (2015) Bone histology in extant and fossil penguins (Aves: Sphenisciformes). *Journal of Anatomy*, 227, 611– 630. https://doi.org/10.1111/joa.12367

Kuehn, A.L., Lee, A.H., Main, R.P. & Simons, E.L.R. (2019) The effects of growth rate and biomechanical loading on bone laminarity within the emu skeleton. *PeerJ*, 7, e7616. https://doi.org/10.7717/ peerj.7616

König, H.E., Korbel, R. & Liebich, H.G. (2016) *Avian anatomy*. Sheffield UK: 5m Publishing Ltd.

Marelli, C.A. & Simons, E.L. (2014) Microstructure and cross- sectional shape of limb bones in great horned owls and red- tailed hawks: How do these features relate to differences in flight and hunting behavior? *PLoS One*, 9, e106094.

McCulloch, G., Aebischer, A. & Irvine, K. (2003) Satellite tracking of flamingos in Southern Africa: the importance of small wetlands for management and conservation. *Oryx*, 37, 480– 483.

Monsarrat, S., Benhamou, S., Sarrazin, F. et al. (2013) How predictability of feeding patches affects home range and foraging habitat selection in avian social scavengers? *PLoS One*, 8, e53077. https://doi. org/10.1371/journ al.pone.0053077.

Muijres, F.T., Johansson, L.C., Bowlin, M.S., Winter, Y. & Hedenström, A. (2012) Comparing aerodynamic efficiency in birds and bats suggests better flight performance in birds [published online ahead of print May 18, 2012]. *PLoS One*, 7, e37335. https://doi.org/10.1371/ journ al.pone.0037335

Norberg, U.M. (1985) Flying, gliding, and soaring. In: Bramble, D.M., Liem, K.F. and Wake, D.B. (Eds.) *Functional Vertebrate Morphology*.
Cambridge MA: Harvard University Press, pp. 129– 158.

Norberg, U.M. (1990) *Vertebrate flight*. Berlin, Heidelberg: Springer.

Norberg, U.M. (1996) Energetics of flight. *Avian energetics and nutritional ecology*. Boston MA: Springer, pp. 199– 249.

Novitskaya, E., Ruestes, C.J., Porter, M.M., Lubarda, V.A., Meyers, M.A. & McKittrick, J. (2017) Reinforcements in avian wing bones: Experiments, analysis, and modeling. *Journal of the Mechanical Behavior of Biomedical Materials*, 76, 85– 96. https://doi. org/10.1016/j.jmbbm.2017.07.020

Nudds, R.L. & Bryant, D.M. (2000) The energetic cost of short flights in birds. *Journal of Experimental Biology*, 203, 1561– 1572.

Nudds, R.L., Dyke, G.J. & Rayner, J.M.V. (2007) Avian brachial index and wing kinematics: putting movement back into bones. *Journal of Zool.*, 272, 218– 226.

Nudds, R.L., Kaiser, G.W. & Dyke, G.J. (2011) Scaling of avian primary feather length. *PLoS One*, 6, e15665. https://doi.org/10.1371/journ al.pone.0015665

Padian, K. (2013) Why study the bone microstructure of fossil tetrapods? In: Padian, K. and Lamn, E.- T. (Eds.) *Bone histology of fossil tetrapods: advancing methods, analysis and interpretation*. California: University of California Press, pp. 1– 11.

Pennycuick, C.J. (2002) Gust soaring as a basis for the flight of petrels and albatrosses (Procellariiformes). *Avian Science*, 2, 1– 12.

Pennycuick, C.J. (2008) *Modelling the flying bird*. Cambridge MA: Academic Press, pp. 1– 5.

Pratt, I.V. & Cooper, D.M.L. (2017) A method for measuring the three- dimensional orientation of cortical canals with implications for comparative analysis of bone microstructure in vertebrates. *Micron*, 92, 32– 38.

Pratt, I.V., Johnston, J.D., Walker, E. & Cooper, D.M.L. (2018) Interpreting the three- dimensional orientation of vascular canals and cross- sectional geometry of cortical bone in birds and bats. *Journal of Anatomy*, 232, 931– 942.

Prinzinger, R., Nagel, B., Bahat, O., Bögel, R., Karl, E., Weihs, D. et al. (2002) Energy metabolism and body temperature in the Griffon Vulture (*Gyps fulvus*) with comparative data on the Hooded Vulture (*Necrosyrtes monachus*) and the White- backed Vulture (*Gyps africanus*). *Journal of Ornithology*, 143, 456– 467.

Proctor, N.S. & Lynch, P.J. (1993) *Manual of Ornithology - Avian structure and function*. New Haven CT: Yale University Press.

Rensberger, J.M. & Watabe, M. (2000) Fine structure of bone in dinosaurs, birds and mammals. *Nature*, 406, 619– 622.

Richardson, P.L., Wakefield, E.D. & Phillips, R.A. (2018) Flight speed and performance of the wandering albatross with respect to wind.
Movement Ecology, 6, 3.

de Ricqlès, A., Meunier, F.J. & Castanet, J. et al. (1991) Comparative microstructure of bone. In: Hall, B.K. (ed.) Bone, Boca Raton FL: CRC Press, chap. 3, pp. 1– 78.

Robinson, C. & Karcher, D.M. (2019) Analytical bone calcium and bone ash from mature laying hens correlates to bone mineral content calculated from quantitative computed tomography scans. *Poultry Science*, 98, 3611– 3616.

Ruxton, G.D. & Houston, D.C. (2004) Obligate vertebrate scavengers must be large soaring fliers. *Journal of Theoretical Biology*, 228, 431– 436.

Sanz- Aguilar, A., Béchet, A., Germain, C. et al. (2012) To leave or not to leave: survival trade- offs between different migratory strategies in the greater flamingo. *Journal of Animal Ecology*, 81, 1171– 1182.

Scacco, M., Flack, A., Duriez, O., Wikelski, M. & Safi, K. (2019) Static landscape features predict uplift locations for soaring birds across Europe. *Royal Society Open Science*, 5, 181440.

Schmitz, A., Ondreka, N., Poleschinski, J., Fischer, D., Schmitz, H., Klein, A. et al. (2018) The peregrine falcon's rapid dive: on the adaptedness of the arm skeleton and shoulder girdle [published online ahead of print June 29, 2018]. *Journal of Comparative Physiology A*, 204, 747– 759. https://doi.org/10.1007/s0035 9- 018- 1276- y

Shamoun- Baranes, J., Bouten, W., van Loon, E.E., Meijer, C. & Camphuysen, C.J. (2016) Flap or soar? How a flight generalist responds to its aerial environment. *Philosophical Transactions of the Royal Society B*, 371, 20150395. https://doi.org/10.1098/rstb.2015.0395

Shamoun- Baranes, J., Leshem, Y., Yom- Tov, Y., Liechti O. (2003) Differential use of thermal convection by soaring birds over Israel. *Condor*, 105, 208– 218.

Simons, E.L.R., Hieronymus, T.L. & O'Connor, P.M. (2011) Cross sectional geometry of the forelimb skeleton and flight mode in pelecaniform birds. *Journal of Morphology*, 272, 958– 971.

Simons, E.L.R. & O'Connor, P.M. (2012) Bone laminarity in the avian forelimb skeleton and its relationship to flight mode: testing functional interpretations. *Anatomical Record*, 295, 386– 396.

Skedros, J.G. & Hunt, K.J. (2004) Does the degree of laminarity correlate with site- specific differences in collagen fibre orientation in primary bone? An evaluation in the Turkey ulna diaphysis. *Journal of Anatomy*, 205, 121– 134.

Skedros, J.G., Knight, A.N., Clark, G.C. et al. (2013) Scaling of Haversian canal surface area to secondary osteon bone volume in ribs and limb bones. *American Journal of Physical Anthropology*, 151, 230– 244.

Starck, J.M. & Chinsamy, A. (2002) Bone microstructure and developmental plasticity in birds and other dinosaurs. *Journal of Morphology*, 254, 232– 246.

Sullivan, T.N., Wang, B., Espinosa, H.D. et al. (2017) Extreme lightweight structures: avian feathers and bones. *Materials Today*, 20, 377– 391.

Thielicke, W. & Stamhuis, E.J. (2018) The effects of wing twist in slow speed flapping flight of birds: trading brute force against efficiency. *Bioinspiration & Biomimetics*, 13, 056015.

Voeten, D.F.A.E., Cubo, J., de Margerie, E., Röper, M., Beyrand, V., Bureš, S. et al. (2018) Wing bone geometry reveals active flight in Archaeopteryx. *Nature Comm.*, 9, 923. https://doi.org/10.1038/ s4146 7- 018- 03296 - 8

Wang, B. & Meyers, M.A. (2017) Seagull feather shaft: Correlation between structure and mechanical response. *Acta Biomaterialia*, 48, 270– 288.

Wang, X., McGowan, A.J. & Dyke, G.J. (2011) Avian Wing Proportions and Flight Styles: First Step towards Predicting the Flight Modes of Mesozoic Birds. *PLoS One*, 6, e28672. https://doi.org/10.1371/ journ al.pone.0028672

Warrick, D., Hedrick, T., Fernández, M.J. et al. (2012) Hummingbird flight. *Current Biology*, 22, 472– 477.

Xirouchakis, S.M. & Andreou, G. (2009) Foraging behaviour and flight characteristics of Eurasian griffons Gyps fulvus in the island of Crete, Greece. *Wildlife Biology*, 15, 37– 52.

Zahedi, M.S. & Khan, M.Y.J. (2007) A mechanical model of wing and theoretical estimate of taper factor for three gliding birds. *Journal of Biosciences*, 32, 351– 361.

Zweers, G.A., de Jong, F. & Berkhoudt, H. (1995) Filter feeding in flamingos (*Phoenicopterus ruber*). *Condor*, 97, 297– 324.